

We are IntechOpen, the world's leading publisher of Open Access books Built by scientists, for scientists

4,800

Open access books available

122,000

International authors and editors

135M

Downloads

Our authors are among the

154

Countries delivered to

TOP 1%

most cited scientists

12.2%

Contributors from top 500 universities



WEB OF SCIENCE™

Selection of our books indexed in the Book Citation Index
in Web of Science™ Core Collection (BKCI)

Interested in publishing with us?
Contact book.department@intechopen.com

Numbers displayed above are based on latest data collected.
For more information visit www.intechopen.com



Compressive Stress Relaxation and Creep Properties of Synthetic Fiber and Regenerated Fiber Assemblies

Yoneda Morihiro and Nakajima Chie

Additional information is available at the end of the chapter

<http://dx.doi.org/10.5772/48546>

1. Introduction

In order to realize comfort environment for sleeping, material property of fiber which consists bedclothes is very important. Compression property of fiber assembly is needed to support human body comfortable, and heat and water transport property is needed to keep micro climate in bedclothes comfortable. In Japan, “futon” has been used for bedclothes, and use of “futon” is divided into mattress to support human body (“shiki-futon” in Japanese) and quilt to cover human body (“kake-futon” in Japanese). Futon consists of futon wadding made from fiber assembly and shell fabrics which covers futon wadding. Cotton fiber has been used for futon wadding use, and wool fiber increases its use for futon wadding recently. Therefore, in Japan, many studies concerning compression properties of futon wadding made from natural fiber such as cotton or wool has been conducted [1-5]. Recently, use of synthetic fiber including polyester for wadding increases because it is light and warm, easy to handle and easy to attach many kinds of functionalities. However, a study on compression properties of synthetic fiber assembly has not been conducted so much.

In this study, therefore, compression properties of fiber assembly made of synthetic and regenerated fiber for futon wadding will be investigated. The reason why we focus our study on compression properties is to explore feasibility of these materials as mattress use. In particular, compression viscoelastic properties such as stress relaxation and creep properties will be carried out in this study, because compression viscoelastic properties have not been carried out systematically in spite of its potential effect on sleeping comfort.

In this paper, results of repeated compression-recovery test, compression stress relaxation test and compression creep test of synthetic and regenerated staple fiber assembly are

reported [6-9]. In addition, results of stress relaxation and creep behaviors of fiber assemblies are analyzed based on non-linear viscoelastic model.

2. Samples of fibers used

2.1. Fiber materials

Twelve kinds of staple fiber materials are used for experiment such as three kinds of polyester fiber with round section, three kinds of polyester fiber with heteromorphic section (w-shaped), one kind of polyester fiber with hollow section, three kinds of Cupra fiber and one kind of Lyocell fiber. Sample code is shown in Table 1, and the details of samples are shown in Table 2. Web made from raw fiber material which is subjected to opening and carding process is used. Fiber assembly is conditioned in constant temperature and humidity room (20°C, 65%RH) over 24 hrs and served for experiment.

Sample code	Detail of sample
WPE-1	Polyester staple fiber with w-shaped heteromorphic section
WPE-2	
WPE-3	
RPE-1	Polyester staple fiber with round section
RPE-2	
RPE-3	
RPE-4	Polyester staple fiber with hollow section
PTT	Polytrimethyleneterephthalate staple fiber
CU-1	Cupra-ammonium (Cupra) staple fiber
CU-2	
CU-3	
LY	Lyocell staple fiber

Table 1. Sample code

2.2. Standard condition for the measurement

Important measurement condition in compression test is fiber volume fraction and maximum compression stress. Standard values for fiber volume fraction and maximum compression stress are estimated as follows. Standard value for fiber volume fraction is 0.025, of which value is estimated from standard size and wadding weight of futon commercially available in Japan. Standard value for maximum compression stress is 2352 Pa, of which value is based on the data that average pressure applied to futon by male adult is about 2.3 kPa. Measurement condition used in this study is determined based on these values of standard condition.

2.3. Sample preparation for fiber assembly

In the case of repeated compression-recovery test and compression stress relaxation test, fiber assembly sample is prepared by filling staple fiber into cylindrical cell made of Acrylic

resin (inner diameter: 54mm, height: 100mm). In this case, setting of fiber volume fraction is important as one of the measurement conditions. Fiber volume fraction Φ_f in cylindrical cell is estimated as follows.

$$\Phi_f = 1.27 \times W/\rho d^2 h \quad (1)$$

where, W : sample weight (g), ρ : specific gravity of fiber (n.d.), d : inner diameter of cell (cm), h : height of cell (cm). Amount of staple fiber estimated by equation (1) is filled uniformly into cylindrical cell, and plastic disk of diameter 50mm is put on the top of fiber assembly. This cylindrical fiber assembly is served as samples to compression test.

Sample code	Fineness (dtex)	Fiber length (mm)	Fiber diameter (μm)	Specific gravity (n.d.)	Percentage of crimp (%)	Apparent young's modulus (kg/mm^2)	Bending rigidity ($\text{gf}\cdot\text{cm}^2$)
WPE-1	1.4	38	24.22 ^{*2}	1.38	14.80	318	5.37 $\times 10^{-5*4}$
			6.27 ^{*3}				2.41 $\times 10^{-7*5}$
WPE-2	1.4	51	24.31 ^{*2}	1.38	34.71	291	4.99 $\times 10^{-5*4}$
			6.78 ^{*3}				3.01 $\times 10^{-7*5}$
WPE-3	2.2	B64 ^{*1}	29.06 ^{*2}	1.38	28.29	297	1.04 $\times 10^{-4*4}$
			8.71 ^{*3}				8.39 $\times 10^{-7*5}$
RPE-1	1.3	38	12.76	1.38	26.70	412	5.36 $\times 10^{-6}$
RPE-2	2.2	51	18.15	1.38	27.24	379	2.02 $\times 10^{-5}$
RPE-3	6.6	51	29.17	1.38	33.33	262	9.31 $\times 10^{-5}$
RPE-4	6.6	51	29.79	1.38	27.59	252	1.34 $\times 10^{-3}$
PTT	1.7	51	15.02	1.38	15.43	154	3.85 $\times 10^{-6}$
CU-1	1.4	38	11.84	1.50	8.79	645	6.22 $\times 10^{-6}$
CU-2	1.4	51	13.73	1.50	15.06	639	1.11 $\times 10^{-5}$
CU-3	2.2	76	15.46	1.50	20.51	475	1.33 $\times 10^{-5}$
LY	7.0	64	33.56	1.50	14.62	359	2.23 $\times 10^{-4}$

Table 2. Details of fiber samples

In the case of compression creep test, fiber assembly of which shape is rectangular prism (10cm square base) is used as sample. Fiber volume fraction Φ_f in rectangular prism is estimated as follows.

$$\Phi_f = W/\rho a^2 h \quad (2)$$

where, W : sample weight (g), ρ : specific gravity of fiber (n.d.), a : length of base (cm), h : height of prism (cm). Amount of staple fiber assembly estimated by equation (2) is served as samples to compression creep test after pre-processing.

3. Experimental measurements

3.1. Repeated compression-recovery test

Repeated compression-recovery behavior is measured using KES-G5 compression tester (Figure 1)(Kato Tech Co.)[6]. The movement of compression and recovery is applied to fiber assembly filled in cylindrical cell by metal plate with area 20cm^2 with constant rate, 1mm/sec . The displacement of metal plate is detected by potentiometer, and the movement is controlled by automatic control. Compression stress is measured by strain gauge attached to metal rod which is connected perpendicular to the metal plate. When compression stress reaches maximum value, P_{max} , the compression movement is turned to recovery one. The test was carried out at four different level of P_{max} , 784, 1176, 2352 and 3528 Pa. Number of repeating cycles of compression and recovery is 31 times. The output of electronic signal of the compression stress and the displacement of metal plate from amplifier is recorded by data logger with constant sampling time, 1 sec, and data processing is carried out using personal computer.

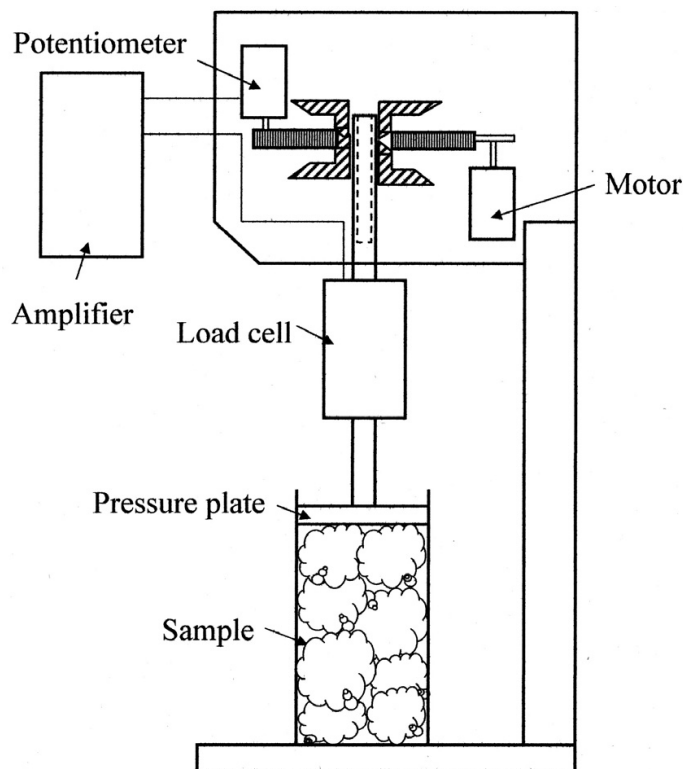


Figure 1. KES-G5 Compression Tester

3.2. Compression stress relaxation test

Compression stress relaxation behavior is measured using KES-G5 compression tester (Kato Tech Co.) on stress relaxation mode [7,8]. Compression displacement is applied to fiber assembly filled in cylindrical cell by metal plate with area 20 cm^2 , and initial height of

sample is fixed at 10cm. Compression stress at this point is regarded as 0. Starting from this point, metal plate is driven downward with speed 5mm/sec to the initial compression displacement, and fixed. Compression stress change at constant displacement is measured from 0 to 10^4 sec with time elapsed. The initial compression displacement is set at five different levels (1, 2, 3, 4 and 5 cm). The output signal of compression stress change is recorded using data logger with sampling time, 1 sec, and the data processing is carried out by personal computer.

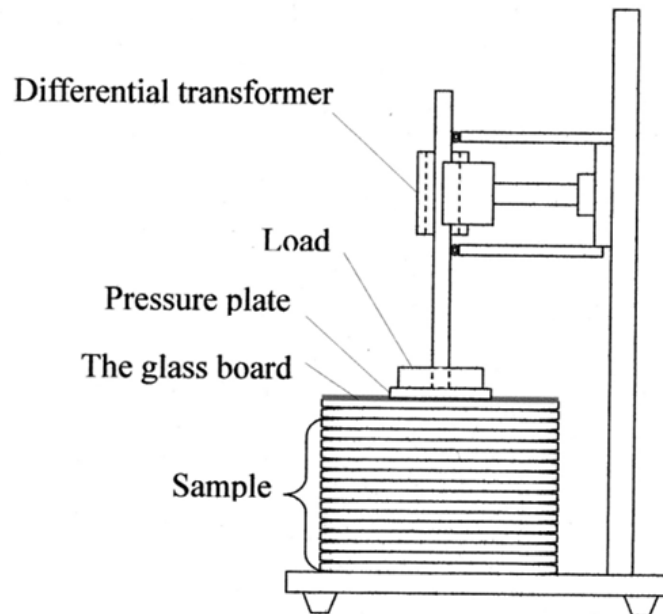


Figure 2. Compression Creep Tester

3.3. Compression creep test

Compression creep behavior is measured using Compression Creep Tester (Figure 2) (Kato Tech Co.)[9]. Metal plate of 10 cm square loaded with constant compression weight is allowed to move downward slowly, and let the metal plate touch to the top of fiber assembly of rectangular prism with 10 cm square. The time when metal plate touches top of sample is taken as 0sec, and measurement of creep starts. Creep deformation is detected by the displacement of metal rod connected perpendicular to metal plate using differential transformer. Creep test is carried out at two different compression load level, 1176 and 2156 Pa. The output signal of creep displacement is recorded by data logger with time elapsed, and data processing is carried out using personal computer. The measurement is carried out from $t=0$ to 10^4 sec. Compression creep rate, R_t (%) is defined as follows,

$$R_t = \varepsilon_t / h_0 \times 100 (\%). \quad (3)$$

where, h_0 : sample height at $t=0$ (sec), ε_t : compression creep displacement (mm) at time t (sec).

4. Results and discussion

4.1. Repeated compression-recovery test

4.1.1. Evaluation method

In general, evaluation of compression properties of fiber assembly (including fabrics) is conducted by characteristic parameters obtained from the measurement of compression-recovery curve as shown in Figure 3. In the case of KES evaluation system, for example, following parameters are used for the evaluation of compression properties [10].

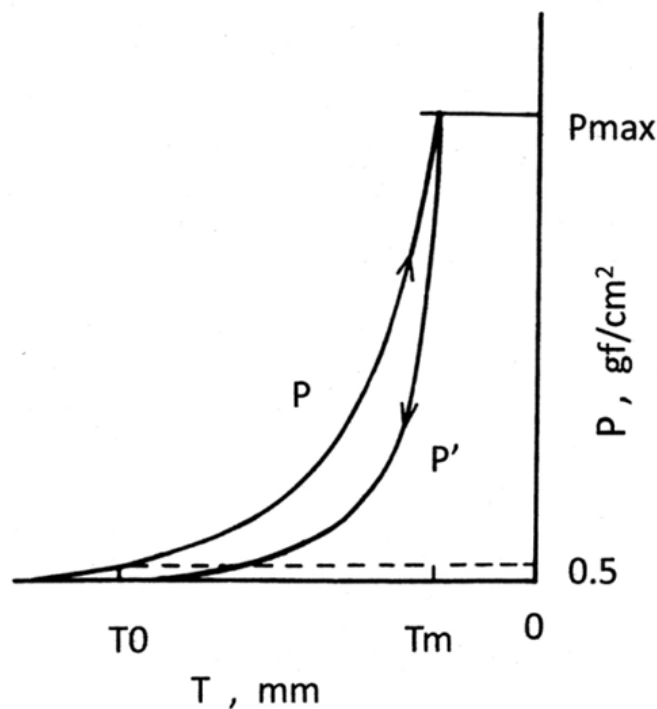


Figure 3. Compression-Recovery Curve

WC: Compressional energy obtained from compression curve P (gf.cm/cm²)

LC: Linearity of compression curve (n.d.)

RC: Compressional resilience (%)

Each parameter is defined as follows.

$$WC = \int_{T_m}^{T_0} PdT \quad (4)$$

$$LC = WC / WOC \quad (5)$$

$$RC = (WC' / WC) \times 100 \quad (6)$$

where, T: Thickness of sample (mm)

T₀: Thickness of sample at P=0.5gf/cm² (mm)

T_m : Thickness of sample at maximum pressure, P_m (mm).

$$WOC = P_m(T_0 - T_m)/2 \quad (7)$$

WC': Recovery energy obtained from recovery curve P'

$$WC' = \int_{T_m}^{T_0} P' dT \quad (8)$$

In the case of evaluating compression properties of fabrics, compression-recovery test is carried out only in one cycle. This is because that natural state of fabrics is generally defined clearly. In contrast, the natural state of three-dimensional fiber assembly is difficult to define, because it does not have specific shape. It is supposed that state of assembly is not uniform and residual stress is still remained for the bulk fiber sample filled in cylindrical cell. In this study, therefore, we try to trace the change of compression properties of sample by repeating a cycle of compression-recovery process for suitable number of cycles. After the investigation of property change with repeating cycles, we will decide in how many cycles are suitable for evaluating compression properties.

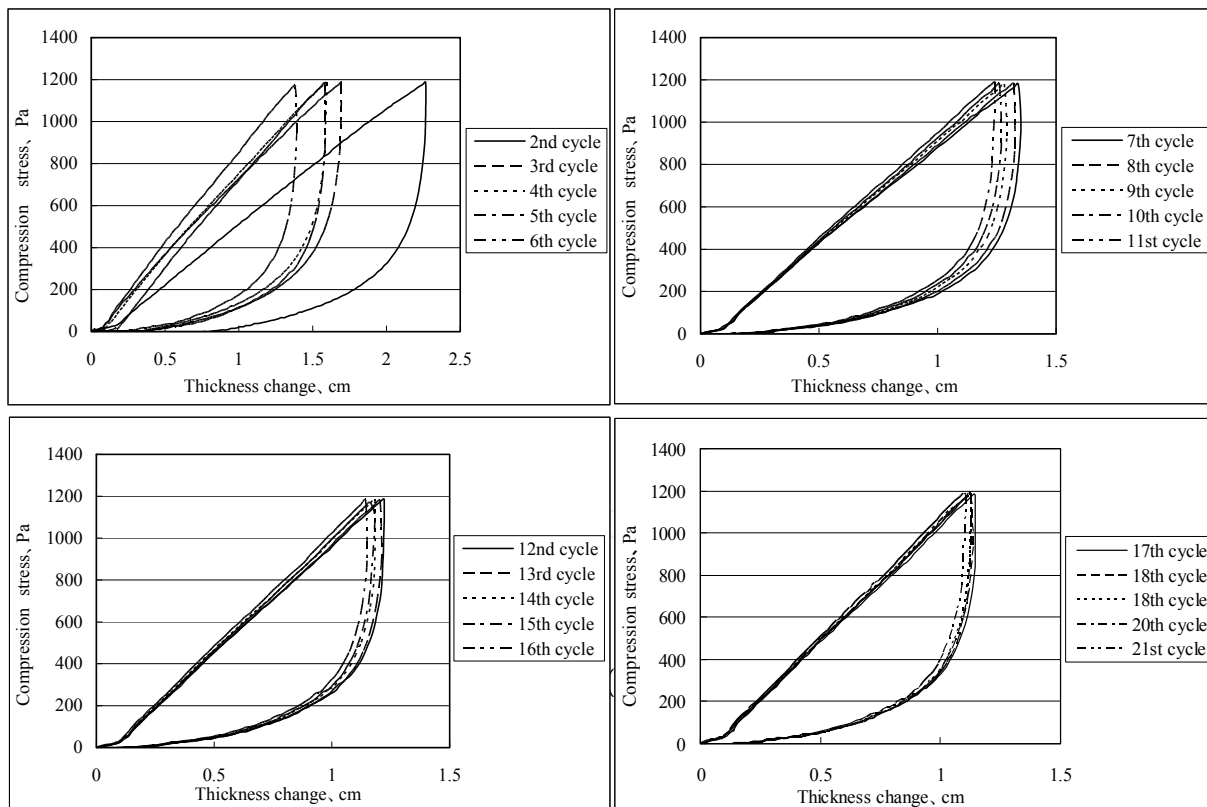


Figure 4. Compression-recovery curve for sample WPE-1

Figure 4 shows the compression-recovery curve in repeated compression test for the polyester staple fiber with heteromorphic section (sample: WPE-1). In this study, the measurement is carried out under the condition that initial fiber volume fraction is 0.0125

for three different levels of maximum compressional stress (784, 1176, 2352 Pa). Each graph includes five cycles of repetition. The data are shown from 2nd cycle to 21st cycle considering nonuniformity of fiber density and residual stress at 1st cycle. Each compression-recovery curve can be distinguished up to 6th cycle, and thereafter the curves have a tendency to overlap each other, and finally difference between each curve is not recognized from 22nd to 21st cycles.

In order to analyze the change of compression-recovery curve against repeating cycles, characteristic parameters, WC , WC' and $T_m - T_0$ per one cycle are obtained. Since WC' and $T_m - T_0$ have the same tendency as WC , results of WC for three samples are discussed in this section.

Behavior of compression energy in compression process, WC is shown in Figures 5,6,7 (sample: WPE-1, RPE-1, CU-1). Characteristic value, WC decreases with increasing repeating cycle, and the degree of decreasing is divided into three stages. At the first stage, from 2nd to 5th cycle, WC decreases rapidly with increasing number of cycles. At the second stage, from 6th to 20th cycles, decrease of WC becomes slowly. At the third stage, from 21st to 31st cycles, WC curve levels off and reaches equilibrium state.

Figures 5,6,7 show results for three different levels of maximum compression stress, P_m , 784, 1176 and 2352 Pa, respectively. From the graph, it is clear that maximum compression stress, P_m influences the relationship between samples in magnitude of WC . When P_m is 784 Pa, WC of PET fiber with heteromorphous section and Cupra fiber is same level, and WC of PET fiber with round section is smaller compared to the others. When P_m is 1176 Pa, WC of Cupra fiber is largest for all cycles, and PET fiber with heteromorphous section follows, and PET fiber with round section is smallest. When P_m is 2352 Pa, magnitude of WC for three samples becomes of the same level for all cycles.

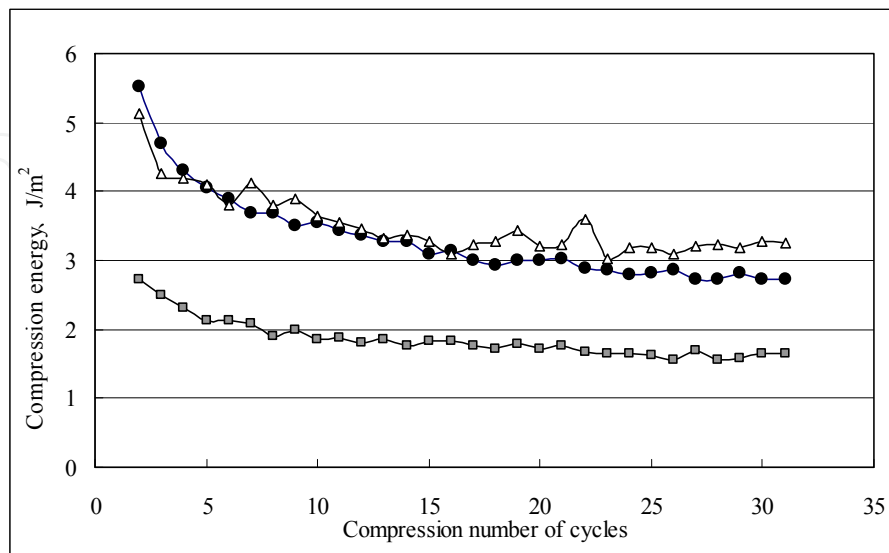


Figure 5. WC vs. Compression number of cycles (784Pa)

Sample: ●:WPE-1, ■:RPE-1, △:CU-1

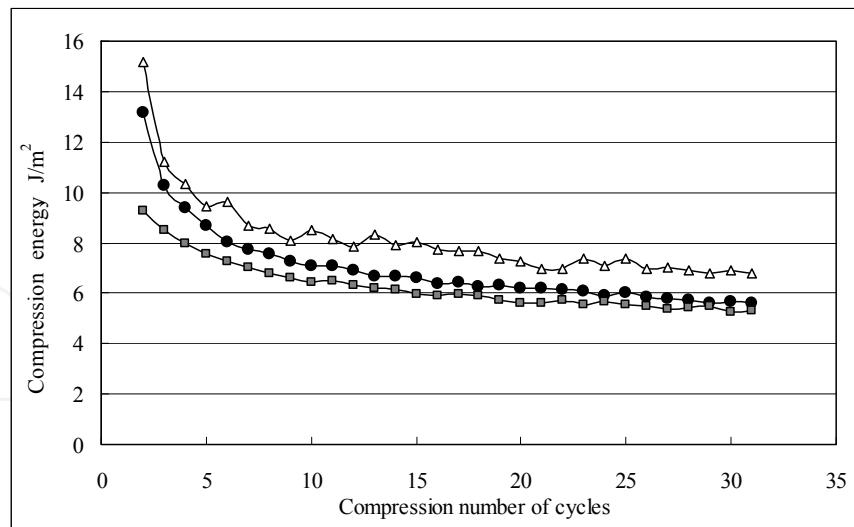


Figure 6. WC vs. Compression number of cycles (1176Pa)

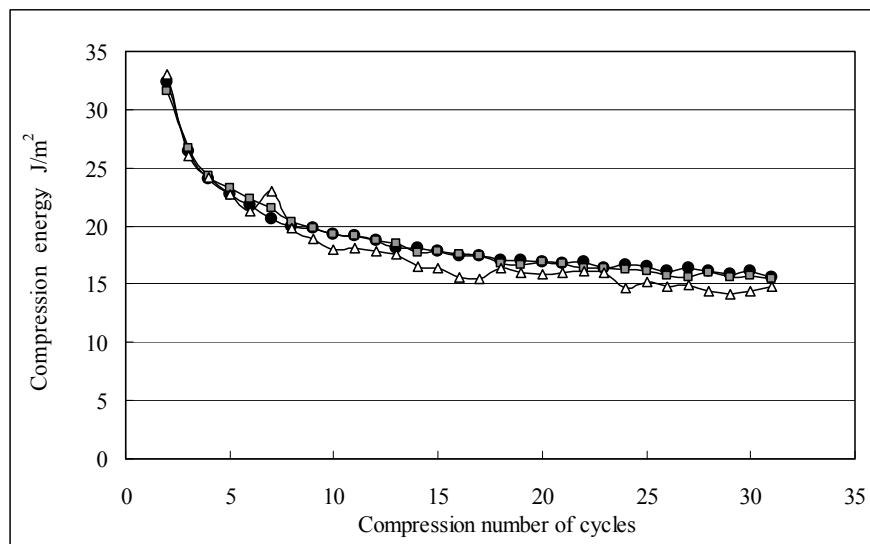


Figure 7. WC vs. Compression number of cycles (2352Pa)

The results show that, in repeated compression-recovery test for fiber assembly, the difference in mechanical parameters between samples appears in some cases or does not in other cases depending on maximum pressure condition. Therefore, in order to characterize the feature in compression properties of fiber assembly, suitable sampling condition in maximum compression pressure must be selected in carrying out compression test.

4.1.2. Analysis by linearizing method

It is confirmed that the feature of compression properties for each sample appears at the 6th cycle of repeated compression-recovery test under the condition of maximum compression pressure, P_m 1176 Pa and fiber volume fraction 0.0125 as discussed in the last section. In this study, the shape of the 6th cycle of repeated compression-recovery curve at the condition mentioned above is analyzed based on linearized method proposed by Kawabata [11].

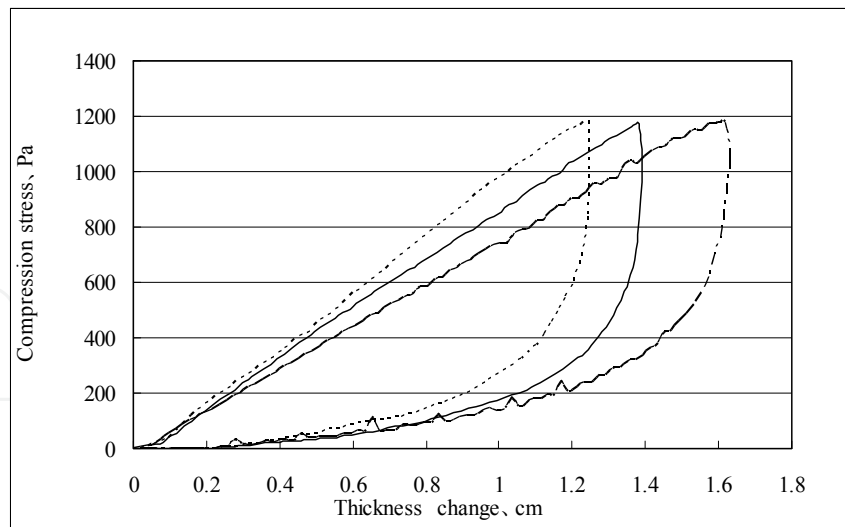


Figure 8. Compression-recovery curve at 6th cycle under the condition that volume fraction is 0.0125 and maximum compression stress is 1176 Pa for three samples.

Straight line: WPE-1

Dotted line: RPE-1

Dots and dashes: CU-1

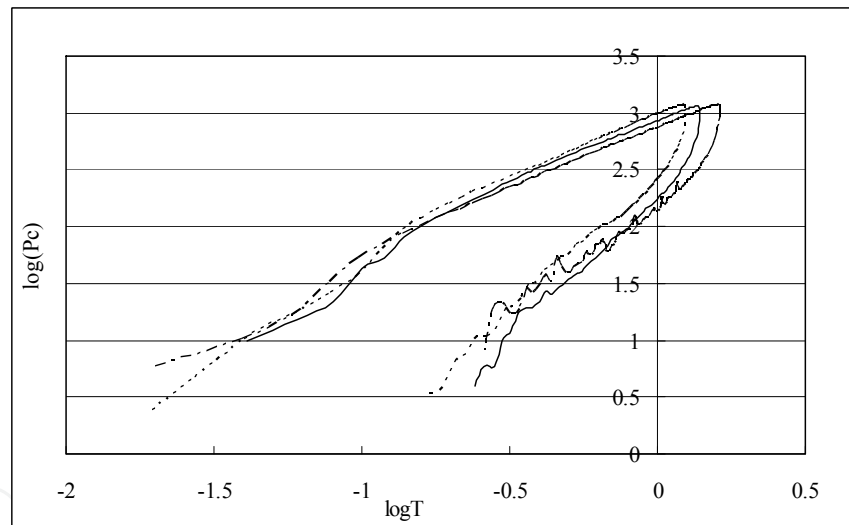


Figure 9. A plot of the relationship between the logarithm of compression stress and the logarithm of thickness change at 6th cycle.

Straight line: WPE-1

Dotted line: RPE-1

Dots and dashes: CU-1

The compression-recovery curves for three samples (WPE-1, RPE-1, CU-1) are shown in Figure 8. The ordinate is compression stress, P_c (Pa), and the abscissa is compression displacement, T (cm). A plot of logarithm of P_c against logarithm of T is shown in Figure 9. It is confirmed that the relationship between $\log P_c$ and $\log T$ is almost linear, and the line has inflexion point both in compression and recovery process. In other words, the relationship between $\log P_c$ and $\log T$ is divided into two stages at a certain point. The range

in which linear relationship holds is summarized in Table 3. The range in which linear relationship at lower stress holds is called as lower stress region, and that of higher stress is called as higher stress region. The relationship between $\log P_c$ and $\log T$ in compression and recovery process is expressed in the following way.

Code	Compression process		Recovery process	
	Low stress area	High stress area	Low stress area	High stress area
WPE-1	0~81.8	81.8~1176	0~27.4	27.4~1176
RPE-1	0~63.7	63.7~1176	0~20.6	20.6~1176
CU-1	0~70.1	70.1~1176	0~30.0	30.0~1176

Table 3. The range where $\log P_c$ - $\log T$ shows linear relationship (unit:Pa)

Parameter	Code	Compression process		Recovery process	
		Low stress area	High stress area	Low stress area	High stress area
n	WPE-1	1.752	1.104	3.553	2.487
	RPE-1	1.727	1.146	2.756	2.213
	CU-1	1.436	1.063	3.097	1.862
A	WPE-1	2275	865	664	182
	RPE-1	2313	984	470	272
	CU-1	1299	740	622	160

Table 4. Parameters n and A

$$\log P_c = \log A + n \log T \quad (9)$$

where, A and n are constants determined by intersection and slope of the curves shown in Figure 9. The A and n depend on mechanical properties of sample, measurement condition and stress region. The values of A and n for three samples and compression and recovery process are summarized in Table 4. Taking equation (9) into account, relationship between compression stress, P_c (Pa) and compression displacement, T (cm) is expressed as follows,

$$P_c = A T^n. \quad (10)$$

The feature of compression-recovery curve can be characterized by parameters A and n.

The effect of properties of fiber on the behavior of compression-recovery curve is investigated. The relationship between parameters A, n and fiber property is different for compression or recovery process and for lower stress region or higher stress region. In the compression process, A and n values depend on such parameter as number of crimp, percentage of crimp and apparent Young's modulus. In the recovery process, A and n values depend on bending rigidity in addition to parameters mentioned above. This fact may support the supposition that the driving force in the recovery process may be bending recovery energy of fiber element.

4.2. Compression stress relaxation test

4.2.1. Residual stress ratio and approximation equation

In this section, functional form of compression stress relaxation behavior for fiber assembly is discussed.

Residual stress ratio S_Y is defined as follows,

$$S_Y = \sigma / \sigma_0, \quad (11)$$

where, σ : stress at time t (Pa), σ_0 : initial stress (stress at $t=0$) (Pa).

Results of measurement of residual stress ratio for all samples are shown in Figures 10~12. Figure 10 shows the results of PET with heteromorph section and PTT, Figure 11 shows that of PET with round and hollow sections, and Figure 12 shows that of Cupra and Lyocell fibers. In each figure, compression displacement is 5 cm. Ordinate is residual stress ratio S_Y (n.d.) in linear scale, and abscissa is natural logarithm of time t (s). As shown in figure, the curve can be approximated by linear function above $t=10^2$ sec for all the samples. Therefore, the curve of residual stress ratio S_Y for $t>10^2$ sec can be expressed approximately as follows,

$$S_Y = K(a_0 - \ln t) \quad (12)$$

where, t : time (s), K , a_0 : constants determined by sample type and measurement condition (n.d.). K and a_0 were determined by least square method based on measurement curve. K values of regenerated fiber assembly are greater than that of synthetic fiber assembly for all displacement conditions. While K values of synthetic fiber range from 0.0075 to 0.0221, K values of regenerated fiber assembly range from 0.0354 to 0.0438. The smaller K value is, the slower compression relaxation speed becomes. It is supposed that synthetic fiber assembly has high sustainability of elasticity and high resistance to compression judging from its small K values. Summarizing these results, evaluation of compression relaxation by K value is very important from the viewpoint of performance in use such as sleeping comfort. It is conjectured that K value is influence by fiber material properties such as number of crimp, crimp percentage, apparent Young's modulus, bending rigidity, inter-fiber friction and viscoelastic properties.

4.2.2. Functional expression for compression stress relaxation of regenerated fiber assembly

In this section, functional expression for compression stress relaxation of regenerated fiber assembly which holds all time regions in this measurement ($0 < t < 10^4$ sec) was discussed.

Compression stress relaxation phenomena for regenerated fiber assembly including Cupra fiber is expressed in the following way [2].

$$S_Y = K \ln \left[\coth \left\{ \frac{1}{2} \left(2e^{-a_0 t} + B \right) \right\} \right] \quad (13)$$

where, K and a_0 are constants determined from equation (2) (n.d.). Constant B can be obtained by substituting $t=0$ and $\sigma=\sigma_0$ into equation (13). Functional expression (13) is derived from the nonlinear two-element viscoelastic model as shown in Figure 13 [12]. This model consists of an elastic element and a Non-Newtonian viscous element. Its viscous behavior is expressed as follows,

$$d\varepsilon / dt = K \sinh(\alpha f) \quad (14)$$

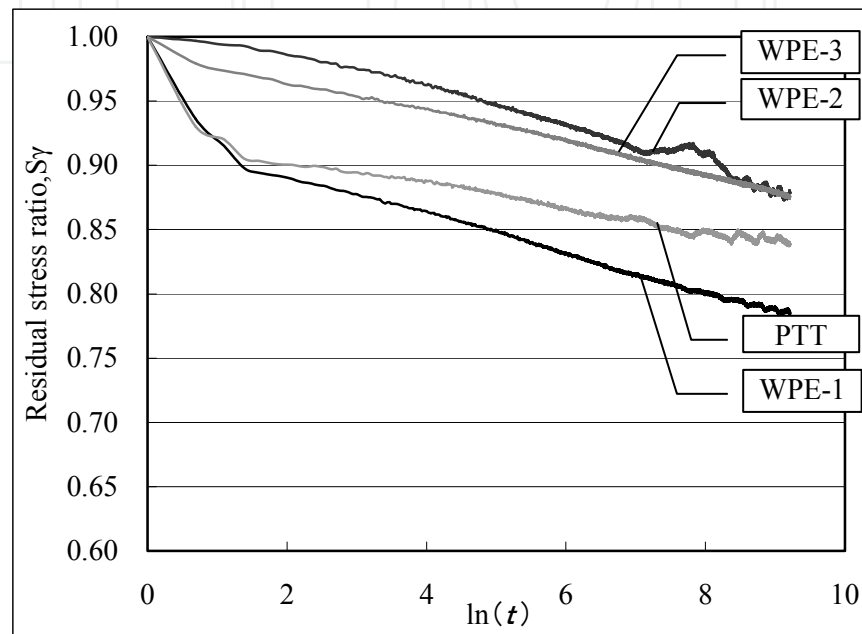


Figure 10. Compression relaxation curve (WPE-1,2,3, PTT, disp.=5cm)

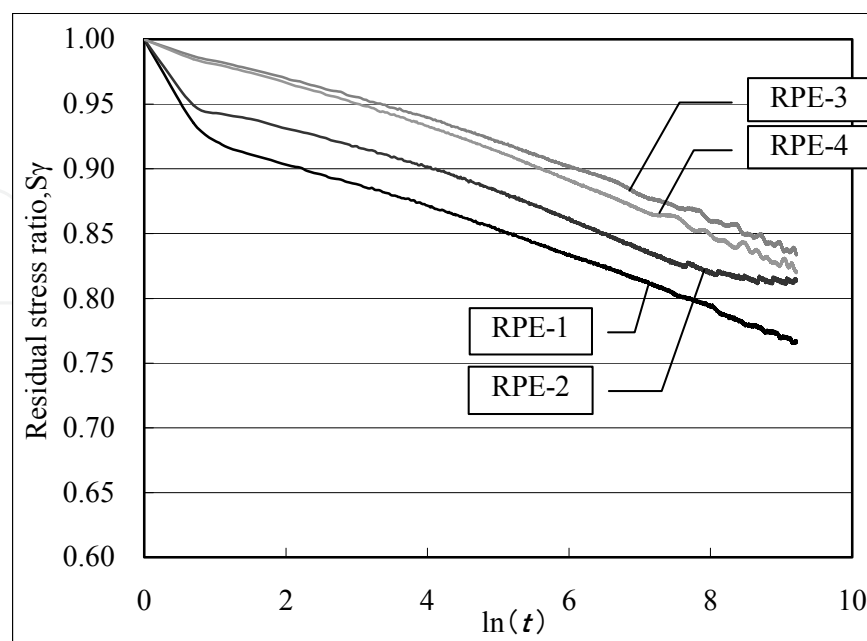


Figure 11. Compression relaxation curve (RPE-1,2,3,4, disp.=5cm)

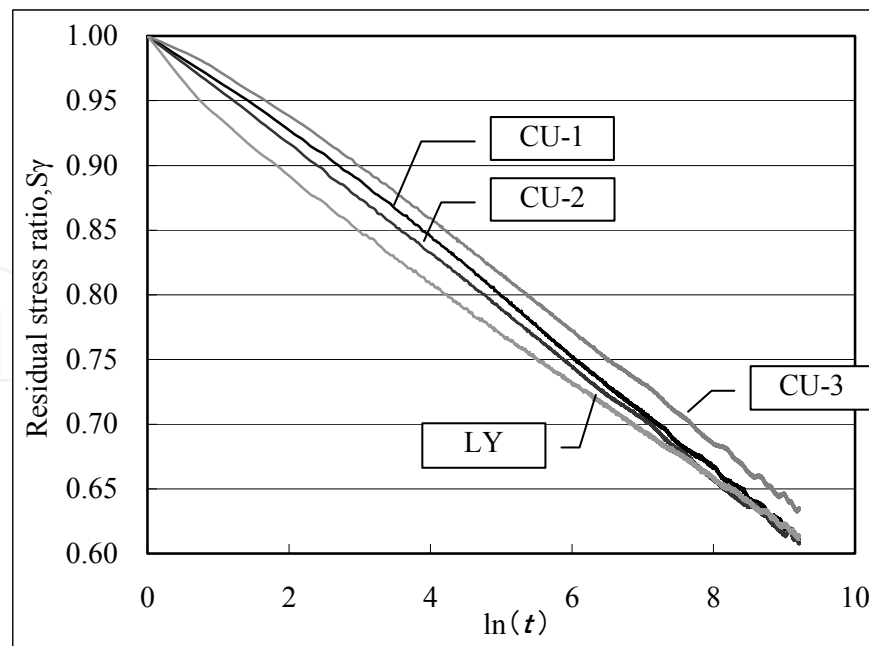


Figure 12. Compression relaxation curve (CU-1,2,3,LY, disp.= 5cm)

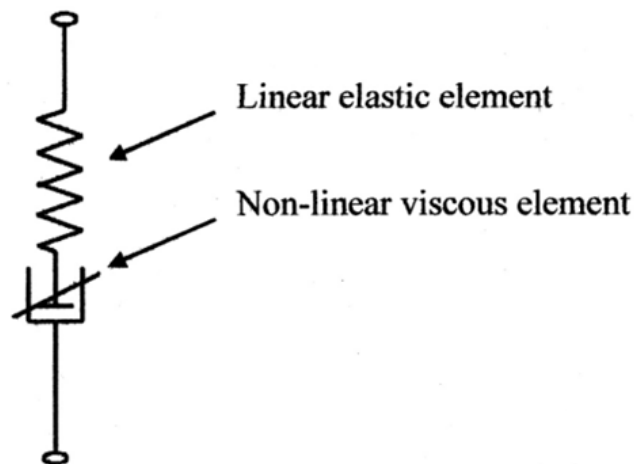


Figure 13. Nonlinear two element model

where, $d\varepsilon/dt$: strain rate, f : force, and K, α : constants concerning non-linear viscous element. The behavior of equation (14) when $f \rightarrow 0$ agrees with that of Newtonian viscosity.

The comparison between calculated curves by equation (13) and measurement curves is shown in Figures 14 and 15. Figure 14 shows the result of Lyocell staple fiber assembly (7dtex, 64mm) (LY) for initial displacement 2 cm. Figure 15 shows the result of Cupra staple fiber assembly (CU-2) for initial displacement 2 cm. In each figure, calculated and measurement curves have good agreement for whole time region. It was known that equation (13) holds for compression stress relaxation phenomena of cotton fiber assembly by Nogai et al [2]. It is confirmed that equation (13) also holds for stress relaxation of cellulosic regenerated fiber assembly such as Cupra and Lyocell fibers in this study.

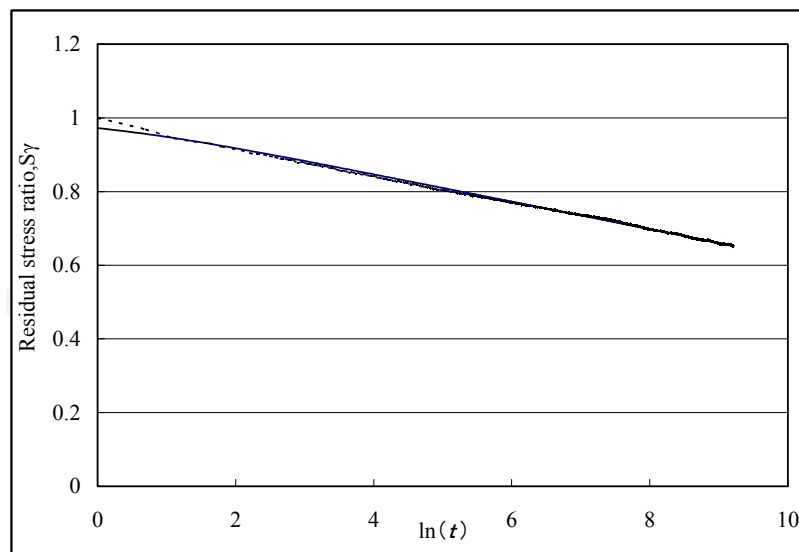


Figure 14. Comparison between experimental and calculated curves (LY) straight line: calculation, dotted line: experimental

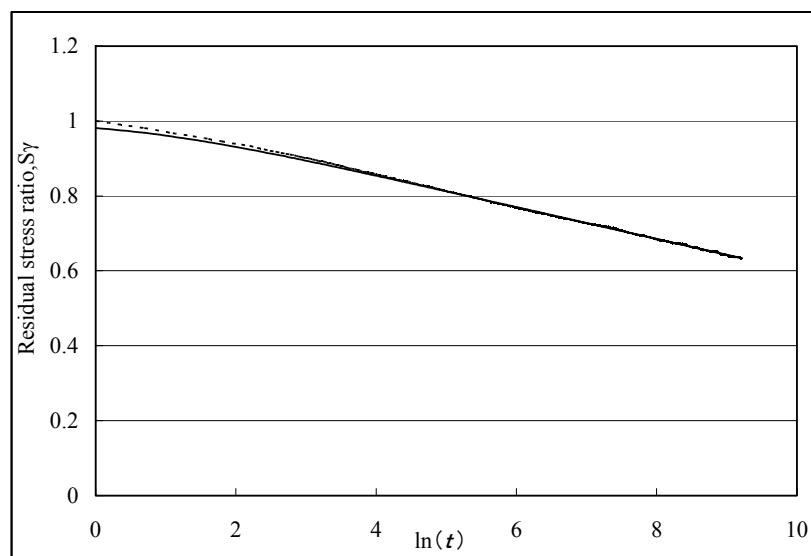


Figure 15. Comparison between experimental and calculated curves (CU-2) straight line: calculation, dotted line: experimental

4.2.3. Functional expression for compression stress relaxation of synthetic fiber assembly

For synthetic fiber assembly, stress relaxation phenomena for whole time region ($0 < t < 10^4$ sec) cannot be expressed by equation (13). This arises from the reason that both type solution cannot be obtained because K values for synthetic fibers are smaller compared to regenerated fibers.

Empirical equation to express compression stress relaxation behavior for synthetic staple fiber assembly is investigated. It is confirmed that linear relationship holds for all samples by bi-logarithmic plot of stress-time curve. Therefore, the empirical equation is obtained as follows,

$$\sigma = \beta t^{-\alpha} \quad (15)$$

where, σ : stress at time t (Pa), t : time (s), and α, β : constants determined by sample type and measurement condition. Agreement of compression stress relaxation curve for synthetic staple fiber assembly with empirical equation (15) is investigated. An example of α and β values for PET with heteromorph section (1.4dtex, 51mm) and fiber volume fraction 0.0139 (WPE-2) is substituted into equation (15). Following equation is obtained.

$$\sigma = 4.68 t^{-0.0164} \quad (16)$$

Comparison between calculated and measurement curves is shown in Figure 16. The agreement of curves calculated by equation (16) with measured curve (WPE-2) is good. As shown in Figure 16, calculated curves are in agreement with measurement curves very well for PET with heteromorph section, PET with round section, PET with hollow section and PTT fibers. (It is hard to distinguish each curve, because the calculated and measured curves show good agreement.)

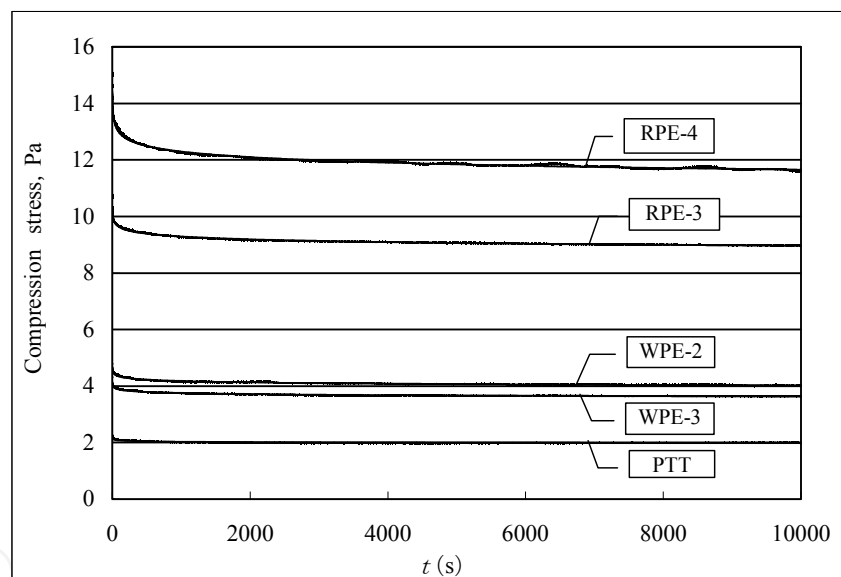


Figure 16. Comparison between experimental and calculated curves using eq.(15)

The relationship between α , β values and fiber volume fraction is shown in Figures 17 and 18, respectively. α value is almost constant against fiber volume fraction. β values increase with increasing fiber volume fraction. β values of PET with round and hollow sections of which count is high and having a tendency to be large.

In the case of synthetic staple fiber assembly, stress relaxation function has a form of decreasing power function with respect to time. This type of relaxation function does not have corresponding viscoelastic model. This is an empirical equation which holds when magnitude and rate in stress relaxation are very small (i.e. elastic deformation).

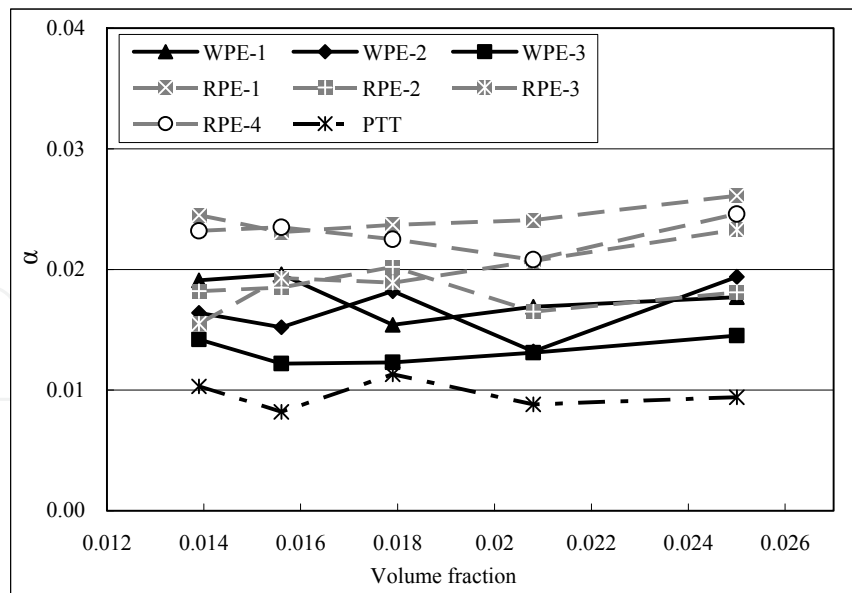


Figure 17. Relationship between α and volume fraction

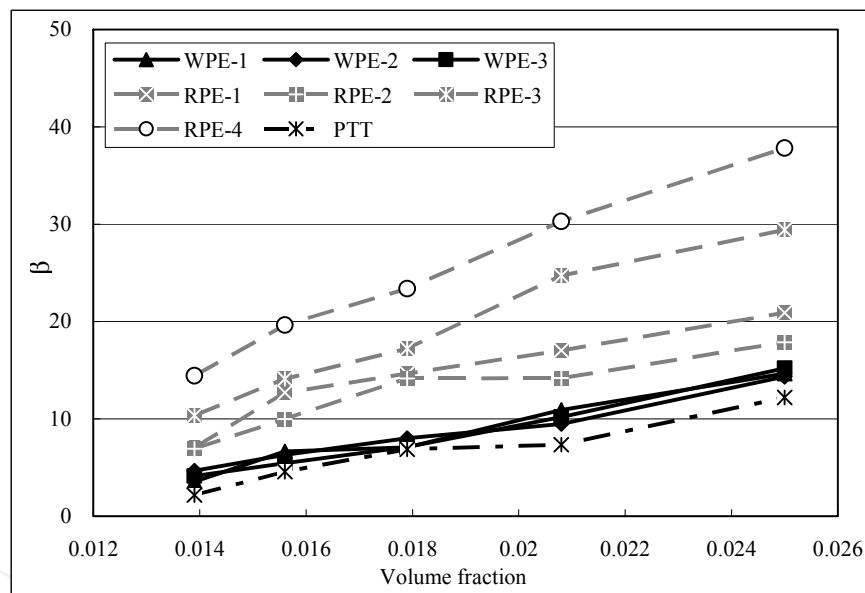


Figure 18. Relationship between β and volume fraction

4.3. Compression creep test

4.3.1. Results of compression creep test

Compression creep test for twelve samples were carried out under low stress condition (1176 Pa) and high stress condition (2156 Pa). Examples of the results for low stress condition are shown in Figures 19~21. Figure 19 shows the result of PET with heteromorphic section and PTT, Figure 20 shows that of PET with round section and hollow section, and Figure 21 shows that of Cupra and Lyocell fibers. The ordinate is compression creep displacement ε (mm), and the abscissa is natural logarithm of time t (s). As seen from

the figure, compression creep curve is almost linear against logarithm of time from 10^1 to 10^4 sec. As for type of fiber material, compression creep displacement of regenerated fiber assembly such as Cupra and Lyocell fibers is greater than that of synthetic fiber assembly.

Compression creep displacement ratio $R_t(\%)$ for different fiber material is investigated. Compression creep displacement ratio R_t at $t=10^4$ sec of regenerated fiber assembly is greater than that of synthetic fiber assembly.

R_t at 10^4 sec for low stress condition is as follows. PET with heteromorphic section (WPE-1, 2, 3) : 0.5 ~ 1.2%, PET with round section (RPE-1, 2, 3) : 1.1~3.2%, PET with hollow section (RPE-4): 1.5%, PTT: 0.8%, Cupra (CU-1, 2, 3): 7.0~8.7% and Lyocell (LY): 10.1%.

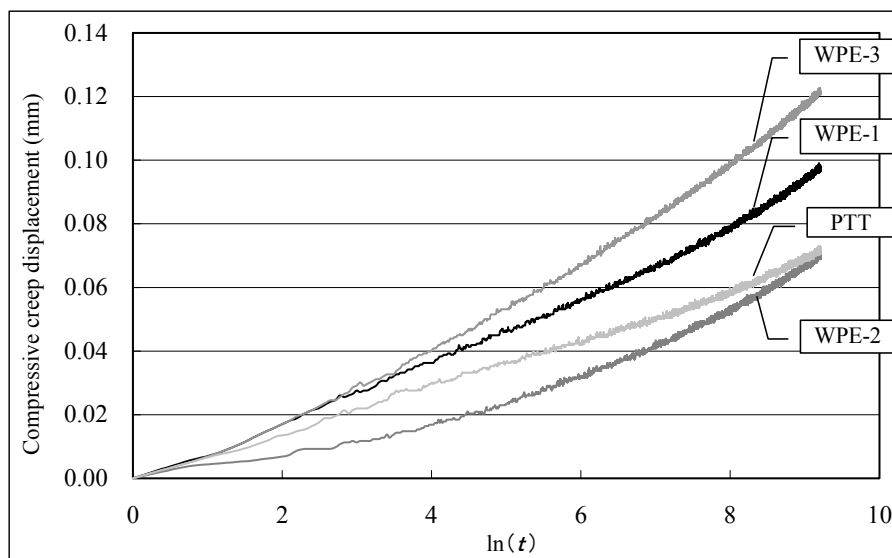


Figure 19. Compressive displacement curve (WPE-1,2,3, PTT)

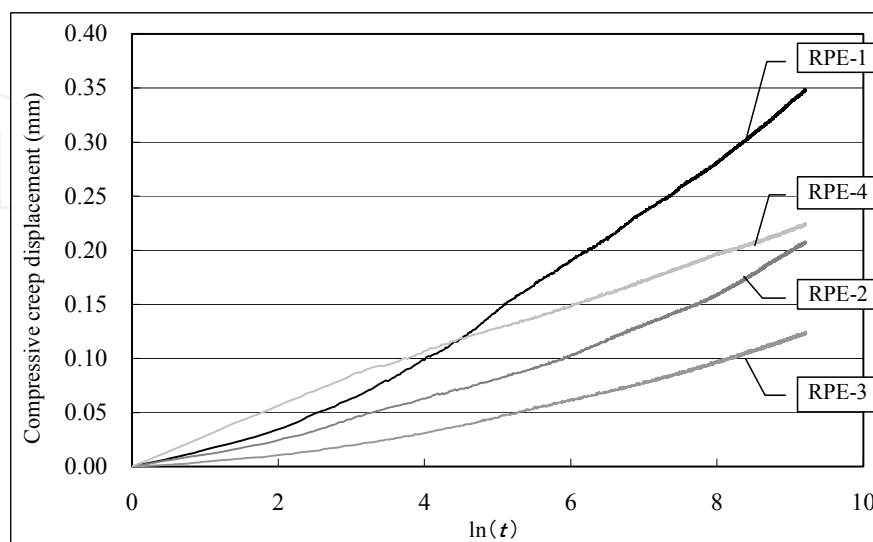


Figure 20. Compressive displacement curve (RPE-1,2,3,4)

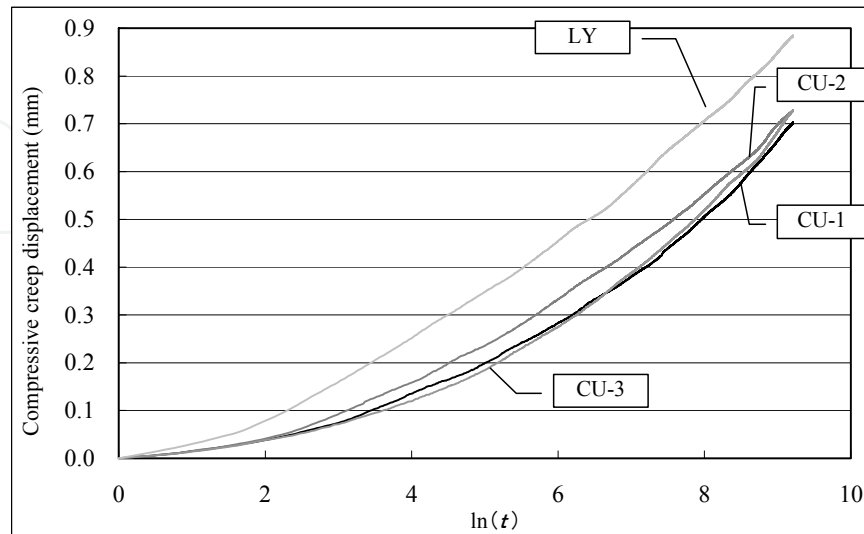


Figure 21. Compressive displacement curve (CU-1,2,3, LY)

Rt at 10^4 sec for high stress condition is as follows. PET with heteromorphic section (WPE-1, 2, 3) : 1.2 ~ 2.2%, PET with round section (RPE-1, 2, 3) : 2.6~4.2%, PET with hollow section (RPE-4): 4.1%, PTT: 1.1%, Cupra (CU-1, 2, 3): 4.9~9.7% and Lyocell (LY): 9.1%.

Creep displacement ratio Rt of samples that have same fineness and same fiber length (1.3 or 1.4 dtex and 38mm) are compared. Rt of Cupra (CU-1) is largest, PET with round section (RPE-1) follows, and PET with heteromorphic section (WPE-1) is smallest. Creep displacement ratio Rt of samples that have same fineness and same fiber length (6.6 dtex and 55mm) are also compared. Rt of PET with round section (RPE-3) is larger than that of PET with hollow section (RPE-4).

In the next place, compression stress dependence of creep displacement is examined. Figure 22 shows Rt values at $t=10^3$ sec for low stress condition (1176 Pa) and high stress condition (2156 Pa). Samples of which Rt at high stress condition are larger than that of low stress condition are as follows; WPE-1, WPE-2, RPE-1, RPE-3 RPE-4 and CU-1. Samples of which stress level dependence is not observed are as follows; WPE-3, RPE-2 and PTT. Samples of which Rt at high stress condition is lower than that of low stress condition are as follows; CU-2, CU-3 and LY. As a result, the behavior of stress level dependence shows different types for different samples. It is conjectured that this phenomena may be arisen from nonlinear viscoelastic behavior in compression creep of fiber assembly.

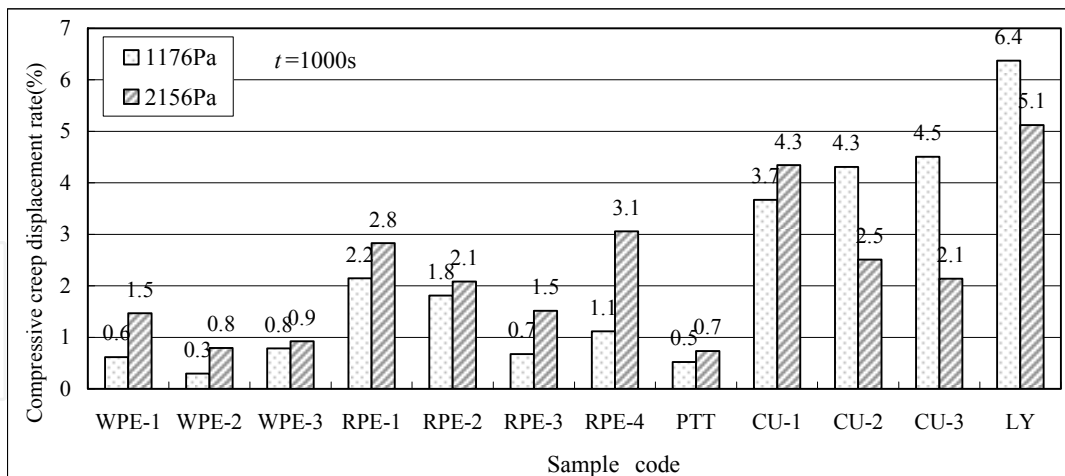


Figure 22. Compressive displacement rate at t=1000s

4.3.2. Functional expression for compression creep behavior

In this section, the equation for compression creep behavior is discussed. Nogai and Narumi[3] showed that following equation holds good for compression creep behavior of cotton fiber mass.

$$\varepsilon_t = Y_0 \ln(vt + 1) \tag{17}$$

where, ε_t : compression displacement (mm), Y_0 (mm) and v (s⁻¹) are constants determined by material properties, measurement condition and compression stress. Equation (17) is derived from non-linear three element viscoelastic model including Eyring viscous element (Figure 23) [12]. In this study, equation (17) is applied to analyze compression creep curve of synthetic and regenerated fiber assembly.

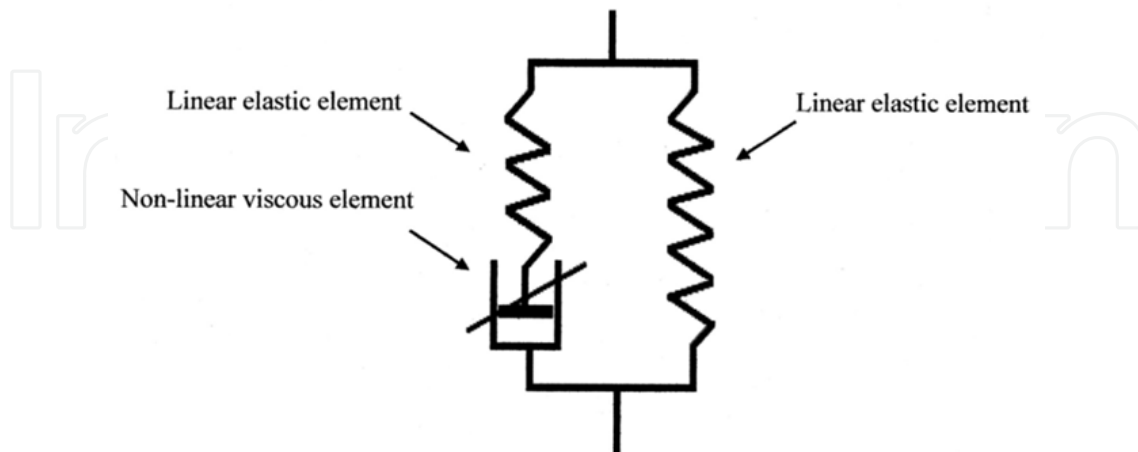


Figure 23. Non-linear three element model

Parameters Y_0 and v are derived from measured curves of compression creep, and the calculated curve is obtained by substituting Y_0 , v values into equation (17). The comparison

between calculated and measured curves is shown in Figures 24~26. Figure 24 shows the result of PET with heteromorphic section (WPE-1), Figure 25 shows that of PET with hollow section (RPE-4), and Figure 26 shows that of Cupra fiber (CU-2). The ordinate in Figures 24~26 is compression displacement ε_t (mm), and the abscissa is time t (s). In each graph, the curves for low stress condition (1176 Pa) and high stress condition are included. Y_0 and v values are obtained as follows. Measured value of ε_t at $t=10^3$ s and $t=10^4$ s are substituted into equation (17), and Y_0 and v are obtained by solving simultaneous equations for $t=10^3$ s and $t=10^4$ s.

As seen from Figures 24~26, the agreement between calculated and measured curves is very well for all samples used in this experiment. Therefore, it is concluded that compression creep behavior of synthetic and regenerated fiber assembly can be well explained by non-linear three element viscoelastic model.

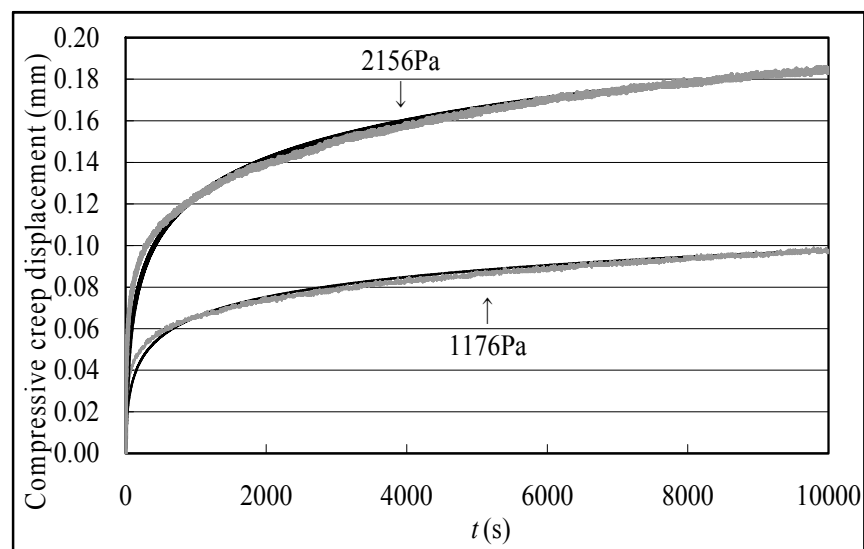


Figure 24. Comparison between experimental and calculated curves using eq(17) (WPE-1)

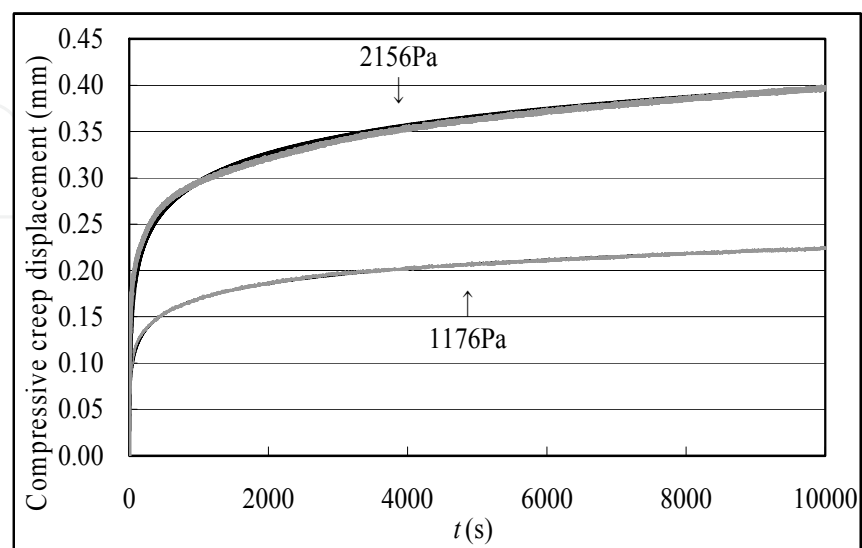


Figure 25. Comparison between experimental and calculated curves using eq(17) (RPE-4)

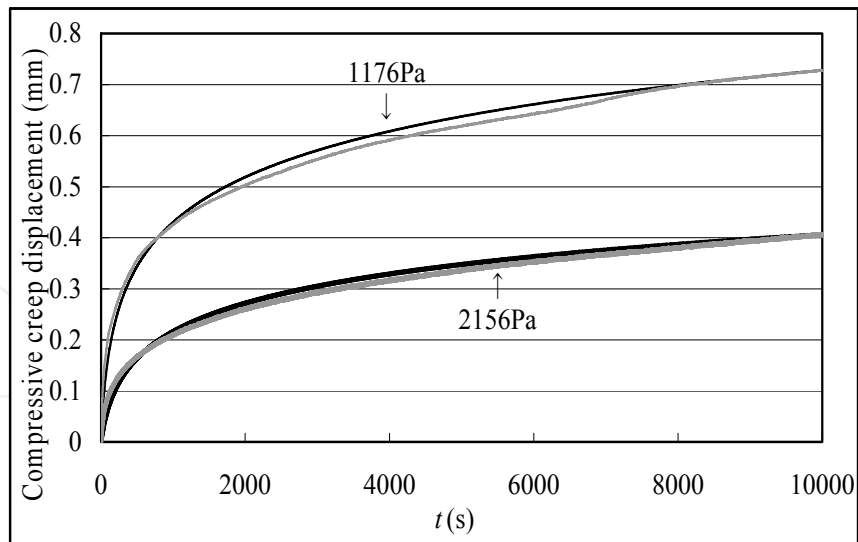


Figure 26. Comparison between experimental and calculated curves using eq(17) (CU-2)

In order to find the relationship between Y_0 , ν values and material properties of fiber, linear regression analysis is carried out. Y_0 has good correlation with apparent Young's modulus, number of crimp and crimp ratio. In particular, correlation between Y_0 and apparent Young's modulus is strong ($R=0.8$). ν has good correlation with bending rigidity ($R=0.95\sim 0.98$).

5. Conclusion

In this study, investigation on compression properties of three-dimensional fiber assembly for futon wadding use is presented. Twelve kinds of synthetic staple fiber assembly and regenerated staple fiber assembly were investigated. KES-G5 compression tester (Kato Tech Co.) is used for the measurement. Repeated compression-recovery test, compression stress relaxation test and compression creep test are carried out. Compression stress relaxation and creep properties of fiber assembly are analyzed based on viscoelastic model. Results are obtained as follows.

i. Repeated Compression-Recovery Test

In order to characterize compression properties of fiber assembly, compression-recovery test with constant strain rate is carried out, and characteristic parameters derived from measured curves are used for evaluation of compression properties. As for the compression measurement of three-dimensional fiber assembly, attention must be paid because fiber assembly does not have specific shape in natural state. To find sampling conditions suitable for characterizing fiber properties, repeated compression-recovery test was carried out for three different levels of maximum compression stress. As a result of sampling, compression-recovery curve at 6th cycles under maximum stress 1176 Pa is selected for the analysis. Linearizing method is applied to the analysis to characterize compression-recovery curve. Functional expression ($P_c=AT^n$) and characteristic parameters A and n are obtained.

ii. Compression Stress Relaxation Test

Two different types of expression for compression stress relaxation function are obtained, approximate expression which holds for long term region and strict expression which holds for whole time region, respectively. Approximate expression of stress relaxation which holds when $t > 10^2$ sec is obtained as follows, $S_Y = K(a_0 - \ln t)$. Stress relaxation rate K of regenerated fiber assembly is larger than that of synthetic fiber assembly. Strict equation of stress relaxation function for whole time region ($0 < t < 10^4$ sec) has two different expressions for regenerated and synthetic fiber assemblies, respectively. In the case of regenerated fiber assembly, strict equation is expressed as follows, $S_Y = K \ln[\coth\{1/2(2e^{-a_0 t} + B)\}]$. Stress relaxation function of coth type is derived from nonlinear two element model including Eyring viscous element. In the case of synthetic fiber assembly, strict equation is expressed as follows, $\sigma = \beta t^{-\alpha}$.

iii. Compression Creep Test

The degree of creep deformation is estimated by creep displacement ratio, R_t (%) at definite time. R_t of regenerated fiber assembly is larger than that of synthetic fiber assembly. The equation for creep displacement, ϵt is obtained as follows, $\epsilon t = Y_0 \ln(vt + 1)$. Creep compliance of \ln type is derived from nonlinear three element model including Eyring viscous element.

The results obtained in this study will be the basic information to design and evaluate fiber materials for futon wadding use with regard to sleeping comfort. Analysis of heat and water transport properties of futon wadding concerning micro climate will be also needed for sleeping thermal comfort.

Author details

Yoneda Morihiko*

Faculty of Human Life and Environment, Nara Women's University, Nara, Japan

Nakajima Chie

Graduate School of Human Culture, Nara Women's University, Nara, Japan

6. References

- [1] Nogai T, Narumi Y (1972) *Senki Ronbunshu* , 25, 180-188
- [2] Nogai T, Narumi Y, Tanaka K (1974) *Senki Ronbunshu* , 27, 177-182
- [3] Nogai T, Narumi Y, Tanaka K (1975) *Senki Ronbunshu* , 28, 77-82
- [4] Yokura H, Sukigara S, Niwa M (1995) *Jpn Res Assn Text End-Uses*, 36, 594-601
- [5] Yokura H, Sukigara S, Niwa M (1996) *Jpn Res Assn Text End-Uses* , 37, 535-543
- [6] Nakajima C, Yoneda M, Itoh Y(2010) *J Text Eng* , 56, 29-38
- [7] Nakajima C, Yoneda M, Itoh Y(2010) *J Text Eng* , 56, 39-46

* Corresponding Author

- [8] Nakajima C, Yoneda M(2010) J Text Eng , 56, 139-146
- [9] Nakajima C, Yoneda M, Nishioka S, Miyazaki A(2010) J Text Eng , 56, 195-202
- [10] Kawabata S (1980) The Standardization and Analysis of Hand Evaluation 2nd ed, The Textile Machinery Society of Japan, Chap.4
- [11] Kawabata S (1986) Senki Ronbunshu , 39, 169-173
- [12] Morton ME, Hearle JWS (1975) Physical Properties of Textile Fibers, The Textile Institute, Chap.18

IntechOpen

IntechOpen